

IRREGULARITIES IN COSMIC RAY COMPOSITION

N. Lund, I. Lundgaard Rasmussen,
B. Peters and N.J. Westergaard

Danish Space Research Institute
Lundtoftevej 7, 2800 Lyngby, Denmark

The relative chemical abundance of some elements in the cosmic radiation can now be investigated over narrow and well defined energy intervals with a precision of the order of a few percent. Variations at this level are to be expected if the presently observable cosmic ray flux contains substantial contributions from a small number of individual sources. With this in mind. We have investigated the relative abundance of B, N, C, and O using data from a recent balloon flight. Significant variations in the element ratios has been determined in the energy interval .5 to 10 GeV/nucleon.

1. Introduction

Most present day models of cosmic ray origin envisage the galactic radiation to consist of the contribution from numerous similar, but not identical sources. The apparent smoothness of the observed energy spectra near earth must then be considered a statistical effect due to superposition of a large number of individual contributions, which tends to obliterate any structural features.

It is conceivable, and even likely, that at anyone time in a particular energy interval the major contribution is due to a relatively small number of sources. It follows that one would expect an analysis of composition carried out with good statistics and very high velocity resolution to exhibit underlying structural features of the cosmic ray spectrum.

As long as isotopic analysis in the relativistic region has not been achieved, these effects are easiest to exhibit for those elements which, by virtue of their high abundance with respect to neighbouring elements contain only few secondary nuclei (i.e. fragments produced during transit). For this reason we have confined our investigation at present to a study of fine structures in the spectra which give rise to variations in the ratio C/O and in an accompanying paper to Fe/Ni.

In each of these ratios we find significant variations with energy/nucleon which, for the reasons given, can not be attributed to cosmic ray propagation (nor to preferential acceleration), but must be attributed to the fact that sources with different abundance ratios make significant contributions to the cosmic ray flux in the rigidity region above ~ 2 GV.

II. Instrument

The preliminary results presented in this paper are based on data obtained during a 60 hour balloon flight carried out in September 1974 from Sioux City, Iowa. More than 250000 primary cosmic ray nuclei was collected during the flight. The results herein are based upon the analysis of $\sim 100,000$ of these.

The data was obtained with the cosmic ray telescope shown in Figure 1. The instrument contains 4 Cerenkov detectors and a flash tube hodoscope. The two PVT counters yield the main charge identification signal. Demanding consistency between the signals in the upper and lower counter we could reject particles destroyed by nuclear interactions during the traversal of the instrument. This rejection is very important due to the amount of matter (10.3 g/cm^2) present in the particle path. The Teflon counter signal and the Aerogel counter signal were used to determine the particle velocity in the range .5-1.9 GeV/n and above 1.9 GeV/n respectively. A more complete description of the telescope will be published in a forthcoming paper.

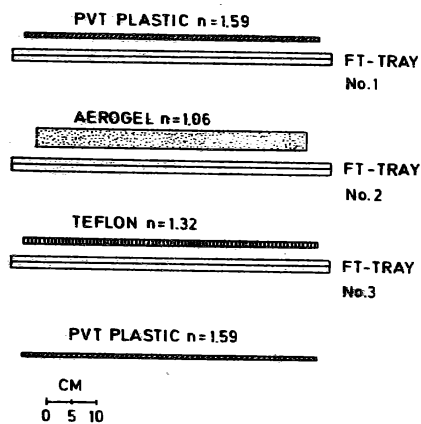


FIG. 1

Detector layout
Geometric factor = $770 \text{ cm}^2 \text{ sterad}$

III. Results

A two dimensional plot of charge vs. velocity is shown in Figure 2. The charge is calculated from the two PVT signals and corrected for saturation due to the scintillation component present in the PVT signal. The Teflon signal and the Aerogel signal plotted is the signal in these two counters divided by the PVT-signal. The saturation in the PVT counter can be seen in the plot from the increase in length of the tracks with charge.

Figure 3 shows the projection on the charge scale of the data shown in Figure 2. The Lithium flux is not shown as the signal threshold used cuts out a part of these particles. It can be seen from the Figure that the charge resolution is excellent over the whole energy range for this set of elements ($\delta Z \sim 0.15$ for $Z = 4-10$, to $\delta Z \sim 0.20$ at $Z = 14$). The resolution is a little better in the high energy region than below 1.9 GeV/n as the Teflon signal is included in the charge determination.

The abundances measured in the instrument and corrected for interactions in the instrument and in the 4 g/cm^2 of overlying atmosphere are shown in table 1.

The number of particles of B, C, N, and O analysed in this paper permits a more detailed study of the flux of these elements as a function of energy. In Table II the flux of B, C, and N relative to O is given. The energy has been determined from the signal in the Teflon counter.

Table I

Observed Events and Abundances Relative to Carbon

Z	Events + uncertainty ¹⁾		Ratio (C=100) corrected to the top of the atmosphere	
	0.5 - 1.9 ²⁾	≥ 1.9	0.6 - 2.0	≥ 2.0
Be	1210 \pm 36	552 \pm 26	10.1 \pm 1.6	9.0 \pm 1.6
B	3212 \pm 58	1333 \pm 38	32.4 \pm 3.2	25.1 \pm 3.2
C	9407 \pm 98	4717 \pm 69	100 \pm 3.1	100 \pm 3.3
N	2651 \pm 52	1364 \pm 38	27.7 \pm 2.3	28.6 \pm 2.4
O	7818 \pm 89	4480 \pm 68	89.7 \pm 1.3	102.6 \pm 1.8
F	225 \pm 18	117 \pm 15	2.0 \pm 0.5	2.1 \pm 0.6
Ne	1207 \pm 36	719 \pm 29	14.0 \pm 0.7	16.8 \pm 0.9
Na	315 \pm 20	153 \pm 16	3.4 \pm 0.5	3.2 \pm 0.6
Mg	1482 \pm 40	912 \pm 32	18.4 \pm 0.6	22.7 \pm 0.9
Al	281 \pm 20	172 \pm 16	3.4 \pm 0.4	4.2 \pm 0.5
Si	1042 \pm 34	708 \pm 28	13.5 \pm 0.5	18.5 \pm 0.8

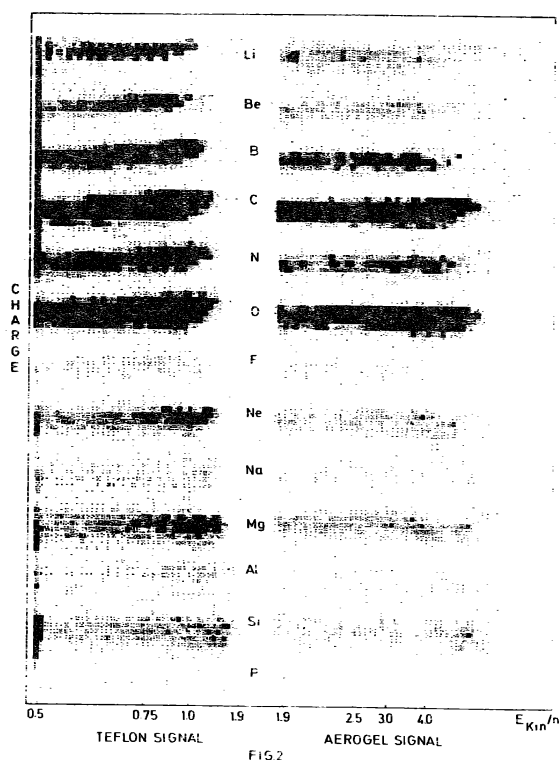
¹⁾The uncertainty includes both statistical uncertainties and the estimated uncertainty in the charge assignment.

²⁾Kinetic energy GeV/c.

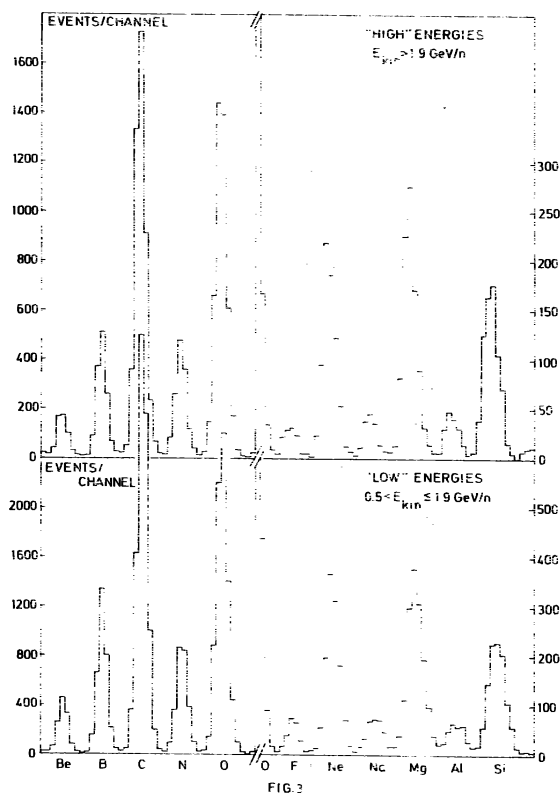
Table II

The Abundance of B, C, and N Relative to O (= 100) as a Function of Energy
Data Corrected to Top of Atmosphere

Kinetic energy MeV/n	B	C	N	N(Calc.)
580- 640	39.6 \pm 3.5	110.9 \pm 6.9	38.7 \pm 3.5	34.4
640- 700	31.9 \pm 2.7	98.2 \pm 5.7	27.9 \pm 2.6	31.6
700- 780	46.0 \pm 3.5	130.7 \pm 7.1	30.3 \pm 2.6	34.5
780- 880	37.7 \pm 2.7	112.0 \pm 5.6	28.0 \pm 2.3	32.8
880-1030	32.7 \pm 2.3	103.8 \pm 4.7	30.7 \pm 2.3	31.0
1030-1250	36.8 \pm 2.3	105.5 \pm 4.6	30.9 \pm 2.2	33.5
1250-1600	33.3 \pm 2.0	96.9 \pm 3.9	30.1 \pm 2.0	33.1
1600-2400	34.2 \pm 1.9	85.2 \pm 3.2	37.3 \pm 2.2	36.7
2400-6700	29.0 \pm 1.6	91.8 \pm 3.1	30.8 \pm 1.8	30.7
> 6700	22.8 \pm 1.3	99.7 \pm 3.3	24.9 \pm 1.5	24.2



Bi-dimensional diagram of the flight data. The black areas contains more than 10 events in a unit square.



Charge histograms corresponding the two energy intervals above and below the aerogel cut off. Note the scale change between oxygen and fluorine.

IV. Discussion

The C/O ratio which we have measured is shown in fig. 4 (top). It varies over the energy interval and the variations are statistically significant.

From the C and O spectra we can calculate those of B and N on the assumptions that:

1. B is produced primarily by the spallation of C and O.
2. N is produced primarily by spallation of O, but contains a small primordial component N
3. The spectrum of the primordial nitrogen component is assumed to be similar to that of oxygen i. e. $N_p(E) = \alpha O(E)$.
4. The relevant spallation cross sections σ_{CB} , σ_{OB} and σ_{ON} are known from laboratory experiments (ref. 1).

- The fraction $\lambda(E)$ of C + O nuclei which have undergone spallation decreases with energy in accordance with results obtained by the Chicago group and others (ref. 2).

Thus

$$B = \lambda(E) (\sigma_{CB} C + \sigma_{OB} O) \qquad N = (\alpha + \lambda(E) \sigma_{ON}) O$$

The calculated ratio N/O is given in the last column of Table II and is in excellent agreement with the measured value over the whole energy range.

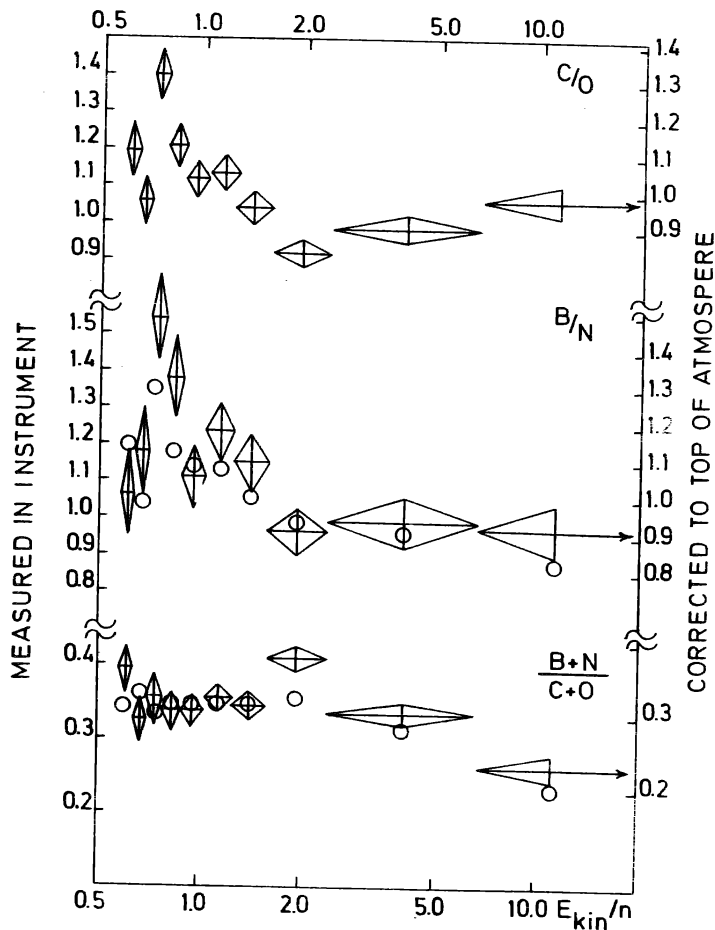


FIG. 4

The abundance ratios C/O (top), B/N (middle) and (B+N)/(C+O) (bottom) as function of energy. The energy scale is based on the signal in the teflon counter. The diamonds are the experimental data, the circles are calculated values as explained in the text.

The calculated ratios B/N and $(B+N)/(C+O)$ are shown by the circles in fig. 4. The experimental values are shown by diamonds. The best fit is obtained for $\alpha = 0.06$.

The agreement between calculation and measurement is good and we conclude therefrom that the observed variation in the C/O ratio is real.

Preferential acceleration in the source and propagation from the source to the earth can, within existing models, not account for the variation in the ratio C/O . We believe that the variation is due to the superposition of sources emitting different cosmic ray spectra with different chemical composition.

V. Acknowledgements

The balloon flight was part of the Saclay-Lyngby Collaboration for HEAO and was supported by the NASA HEAO project. We are indebted to our French collaborators for providing us with the Aerogel radiator and for support during the balloon campaign. We are also indebted to the NCAR launch team which put much effort into assuring the success of the flight.

References

1. Lindstrom, P. J., Greiner, D. E., Heckman, H. H., Cork, B., and Bieser, F. S. LBL-3650 Preprint 1975
2. Juliusson, E., Meyer, P., and Müller, D. Phys. Rev. Lett., 29, 445 (1972).